Title Page

Abnormal Cardiac Formation in Hypertrophic Cardiomyopathy

- Fractal Analysis of Trabeculae and Prephenotypic Gene Expression*

**This work is short-listed for the 2013 AHA Scientific Sessions CVRI Melvin Judkins Young Investigator Award to be presented 17th November 2013*

Captur, Trabeculae in hypertrophic cardiomyopathy

Authors

Gabriella Captur[1,2] MD, MRCP, MSc, Luis Lopes[1,2] MD, Vimal Patel[1,2] MD, MRCP, Chunming Li[3] PhD, Paul Bassett[2,4] MSc, Petros Syrris[1,2] PhD, Daniel M Sado[1,2] MRCP, BSc BM, Viviana Maestrini[1,2] MD, Timothy J Mohun PhD,[5] William J McKenna[1,2] MD, FACC, FRCP, Vivek Muthurangu[2,6] MD, MRCP, Perry M Elliott[1,2] MD, FRCP, FESC, FACC, James C Moon[1,2*] MD, MRCP.

Institutions

[1] **The Heart Hospital**, Division of Cardiovascular Imaging, part of University College London NHS Foundation Trust, 16-18 Westmoreland Street, London W1G 8PH, **UK**

[2] **UCL Institute of Cardiovascular Science**, University College London, Gower Street, London WC1E 6BT, **UK**

[3] **University of Pennsylvania**, Department of Radiology, 3600 Market Street, Suite 380, Philadelphia, PA 19104, **USA**

[4] **Biostatistics Joint Research Office**, University College London, Gower Street, London WC1E 6BT, **UK**

[5] **Developmental Biology Division, MRC National Institute for Medical Research**, The Ridgeway, Mill Hill, London NW7 1AA, **UK**

[6] **UCL Centre for Cardiovascular Imaging and Great Ormond Street Hospital for Children** (GOSH), London WC1N 3JH, **UK**

Correspondence

Dr James Moon,

The Heart Hospital,

16 –18 Westmoreland St,

London W1G 8PH, United Kingdom.

E-mail: james.moon@uclh.nhs.uk Phone No:+44 2034 563 081 Fax No: +44 2034 563 086

Word Count: 5,886

Subject Codes [6], [30], [104]

Abstract

Background: Mutations in genes coding for sarcomeric proteins cause hypertrophic cardiomyopathy(HCM). Subtle structural abnormalities of the myocardium may be present in gene mutation carriers without hypertrophy(G+LVH−) but are difficult to quantify. Fractal analysis has been used to define trabecular complexity in LV noncompaction and to identify normal racial variations. We hypothesized that trabeculae measured by fractal analysis of cardiovascular magnetic resonance(CMR) images are abnormal in G+LVH− patients providing a prephenotypic marker of disease in HCM.

Methods and Results: CMR was performed on 40 G+LVH− patients(33±15yrs, 38%men), 67 patients with a clinical diagnosis of HCM(53±15yrs, 76%men; 31 with a pathogenic mutation(G+LVH+)) and 69 matched healthy volunteers(44±15yrs, 57%men). Trabeculae were quantified by fractal analysis of cine slices to calculate the fractal dimension(FD)-a unitless index of endocardial complexity calculated from endocardial contours after segmentation. In G+LVH− patients apical LV trabeculation was increased compared to healthy volunteers(maximal apical FD, 1.249±0.07 *vs* 1.199±0.05, *P*=0.001). In G+LVH+ and G−LVH+ cohorts, maximal apical FD was greater than in healthy controls(*P*<0.0001) irrespective of gene status(G+LVH+:1.370±0.08; G−LVH+:1.380±0.09). Compared to healthy volunteers, G+LVH− patients also had a higher frequency of clefts(28 *vs* 8%, *P*=0.02), longer anterior mitral valve leaflets(23.5±3.0 *vs* 19.7±3.1mm, *P*<0.0001), greater septal systolic wall thickness(12.6±3.2 *vs* 11.2±2.1mm, *P*=0.03), higher ejection fraction(71±4 *vs* 69±4 %, *P*=0.03) and smaller end-systolic volumes(38±9 *vs* 43±12mls, *P*=0.03).

Conclusions: Increased myocardial trabecular complexity is one of several prephenotypic abnormalities in HCM sarcomere gene mutation carriers without LVH.

Keywords

Hypertrophic cardiomyopathy, Trabeculation, Genetics

Text

Background

Hypertrophic cardiomyopathy (HCM) is the commonest inherited cardiac disease, with a prevalence of 1 in 500 in the general population.[1] It is defined by the presence of left ventricular hypertrophy (LVH) in the absence of abnormal cardiac loading conditions[2] and is predominantly caused by autosomal dominant mutations in sarcomeric protein genes.[3,4] The penetrance of sarcomeric protein mutations is typically incomplete with variable age-related clinical expression. This means that many individuals who carry a causative mutation have no LVH and thus may be falsely reassured when they can still go on to manifest HCM with time.

Subtle structural cardiac abnormalities (elongation of the anterior mitral valve leaflet[5] (AMVL), clefts[6–8]) may be present in mutation carriers without LV hypertrophy[9] (G+LVH−) imaged by cardiovascular magnetic resonance (CMR) (Figure 1) but are non-specific. Semi-quantitative methods have suggested that myocardial trabeculae are abnormal in clinically overt HCM[10,11] but trabecular anatomy in prephenotypic mutation carriers has not been evaluated. Fractal analysis has been used to define myocardial trabecular complexity in individuals with left ventricular noncompaction and to identify normal racial variations.[12] We hypothesized that trabecular complexity determined by fractal analysis of standard CMR images is abnormal in HCM mutation carriers without LVH and provides a prephenotypic marker of disease.

Methods

Study population

One-hundred-and-seven individuals (aged 15 - 82 years) from 97 unrelated families with HCM recruited from a dedicated cardiomyopathy clinic at The Heart Hospital, UCLH, London were studied between January 2007 and February 2013: G+LVH− (*n* = 40); G+LVH+ (*n* = 31) and G–LVH+ (*n* = 36). Age (+/- 8 years), gender, body surface area (+/- 10%) (BSA) and ethnicity-

matched healthy volunteers were recruited for comparison with the three HCM groups, with some healthy volunteers being matched to patients in more than one group (n = 69, 44 ± 15 years).

Inclusion criteria for G+LVH− patients were: i) maximal LV wall thickness <13 mm by CMR and mass within the normal range relative to BSA, age and gender; ii) sinus rhythm, no LVH and no pathological Q waves/T-wave inversion on 12-lead electrocardiography (ECG); iii) no causes of secondary LVH (valve disease, hypertension). Diagnosis of HCM in the LVH+ groups was based on demonstration by CMR of a nondilated, hypertrophied LV (maximum wall thickness ≥15 mm) in the absence of another cardiac or systemic disease that could produce the magnitude of hypertrophy.[1] Exclusion criteria included: evidence of substantial LV remodeling and the end-stage phase of HCM, previous alcohol septal ablation, surgical septal myectomy or mitral valve replacement. Healthy volunteers had no history of cardiovascular disease or hypertension, a normal physical examination, no family history of inheritable cardiomyopathy or sudden cardiac death and no personal history of unexplained syncope. Exclusion criteria for all participants were the presence of conventional contra-indications for CMR, claustrophobia and a high arrhythmogenic burden (e.g. atrial fibrillation, frequent ectopics) that precluded good cine acquisitions by retrospective gating.

An ethics committee of the UK National Research Ethics Service approved the generic analysis of anonymized clinical scans. The genotyping project was approved by the UCL/UCLH Joint Research Ethics Committee. At the time of enrolment all participants gave written informed consent conforming to the declaration of Helsinki (V. revision, 2000).

Electrocardiography

Standard 12-lead ECG was performed in the supine position during quiet respiration. LVH was evaluated with the Romhilt-Estes[13] and electrocardiographic European criteria.[14,15] ECGs were analyzed by an experienced observer blinded to clinical information.

Genetic screening

Blood samples were collected at initial evaluation and genomic DNA was isolated from peripheral blood lymphocytes, using standard methodology. All G+LVH+ and G−LVH+ cases were screened using a targeted high-throughput sequencing methodology and sequencing data was subjected to bioinformatics analysis as previously described.[16] Briefly, 2.1 Mb of genomic DNA sequence was screened per patient, covering coding, intronic and selected regulatory regions of 41 cardiovascular genes. Solution-based sequence capture was used followed by massive parallel resequencing on Illumina GAIIx. Average read-depth in the 2.1 Mb target region was 120. For G+ cases, non-synonymous pathogenic and likely pathogenic variants were selected on frequency (<0.5% based on the 1000 Genomes Database[17]) and putative functional consequence: either missense variants previously published to be associated with the disease or splicing, nonsense and frameshift variants.[16] G+ individuals were defined as the ones carrying a mutation in one of the following sarcomere genes: myosin binding protein C (*MYBPC3*), beta myosin heavy chain (*MYH7*), troponin T (*TNNT2),* troponin I (*TNNI3),* myosin regulatory light chain (*MYL2*), myosin essential light chain (*MYL3),* tropomyosin (*TPM1*) and cardiac alpha actin (*ACTC1*). Thick-filament mutations consisted of *MYBPC3, MYH7, MYL2* and *MYL3,* while thin-filament mutations included *TNNT2, TNNI3, TPM1* and *ACTC1*.

Cardiovascular magnetic resonance

Standard clinical scans (localizers, three long-axis views, black and white blood images, full LV short-axis stack) were performed using a 1.5-T magnet (Avanto, Siemens Medical Solutions, Erlangen, Germany). CMR short-axis volumetric studies[18] were acquired from retrospectively-gated, breath-held, balanced, steady-state free-precession cines (slice thickness, 7.0 mm; inter-slice gap, 3.0 mm; flip angle, 60 - 80°; TR, 3.0 ms; TE, 1.33 ms; FOV read typically, 380 mm; phase resolution, 75%; typical acquired voxel size 1.5 x 1.7 mm; lines per segment, 12).

Non-fractal image analysis

LV volumes, ejection fraction (EF) and LV mass were determined according to standardized CMR methods[19] (papillary muscles were included in the LV mass). LV wall thickness was calculated for the septum and posterior wall on end-diastolic and end-systolic short-axis cine frames. End-systolic left atrial areas were measured by planimetry on 4-chamber view. AMVL length was measured using the method described by Maron et al.[5] The three long-axis views and a modified 2-chamber view (transecting right ventricular insertion points) were evaluated for the presence of myocardial clefts defined as focal myocardial defects with a depth of ≥50% of the adjacent myocardium.[8] The degree (%) of transmural penetration of clefts was recorded. Presence of rest LV outflow tract obstruction and systolic anterior motion of the mitral valve leaflet were noted. Breath-held, delayed contrast enhancement images acquired through an inversion recovery turbo Fast Low Angle Shot (FLASH) sequence were obtained 7-15 min after injection of 0.1 mmol/kg gadolinium-DTPA. The presence of fibrosis and the structure of the LV were evaluated by cardiologists experienced in CMR (J.C.M, G.C., D.S.).

Fractal analysis

Fractal analysis was performed on the end-diastolic frames of each short-axis cine slice in the LV stack using our in-house, semi-automated MATLAB® graphical user interface (The MathWorks Inc., Natick, MA, USA; authors – V.Mu, C.L., G.C.). CMR slices underwent automatic scaling according to DICOM pixel spacing metadata as the first image processing step. Analysis typically took <4 minutes per heart and was divided into three parts (Figure 2): 1) user-defined selection of the region-of-interest (ROI), 2) image segmentation to extract the endocardial border and 3) calculation of the fractal dimension (FD) of all endocardial borders in the LV stack using a standard box-counting method as previously described by our group.[12] A validated, region-based level set method[20] was employed for blood-endocardial segmentation and bias field estimation and correction of CMR data. Intracavitary papillary muscles and parts of the subvalvular apparatus also provided edges to the final

image submitted to fractal analysis. The most apical ventricular slice which is known to be prone to partial voluming, was excluded from fractal analysis.

To assess the global LV FD, an average of all FD in the LV stack was measured. To assess local fractal characteristics, the LV stack was split into basal and apical halves (consistently discarding the median slice in unevenly numbered stacks). Mean and maximal values for basal and apical FD were then calculated. Validation and repeatability experiments for the fractal algorithm are described in the Online Supplementary Material.

Statistical analysis

Statistical analysis was performed in R programming language for statistical computing (version 3.0.1, The R Foundation for Statistical Computing) and in SPSS for Windows version 20.0 (Chicago, IL, USA). Descriptive data are expressed as mean ± standard deviation (s.d.) except where otherwise stated. Distribution of data was assessed on histograms and using Shapiro-Wilk test. Categorical variables were compared by χ^2 tests. Correlation between continuous variables was assessed with Pearson's Correlation Coefficient. FD of HCM groups and matched healthy volunteers were directly compared using paired *t*-Test. Linear regression was used to determine which variables were associated with LV trabeculation across the three HCM groups. To adjust for differences when comparing between individual HCM groups a multivariate model was fitted which included variables identified as statistically significant in the univariate analyses. An optimal threshold value for FD within this case-control population was calculated as the Youden Index derived from the area under the receiver operating characteristics curve. Paired measurements for repeatability of fractal analysis were evaluated using the Bland-Altman method. Intraclass correlation coefficient was used to compare variability within and between readers. A two-sided *P* value <0.05 was considered significant.

Results

Patient characteristics

HCM groups were matched with equivalent healthy volunteers in terms of age, gender and body surface area (Table 1). Patients with hypertrophy were nearly 2 decades older than the G+LVH− group. Children and adolescents (<18 years) comprised 20% of the G+LVH− cohort. Of the 40 G+LVH− patients, 1 subject was excluded from subsequent analysis on account of maximal LV wall thickness by CMR >13 mm, not previously noted at echocardiography. Fifty-four unique mutations (29 unique mutations in the G+LVH+ plus 25 from the G+LVH−), in a total of 6 sarcomere genes were represented across the G+ populations (a full listing is provided in Supplementary Tables 1 and 2): *MYBPC3*, *n*=29, *MYH7*, *n*=20, *MYL2*, *n*=1, *TNNT2*, *n*=7, *TNNI3*, *n*=11 and *ACTC1*, *n*=2, with mutations in *MYBPC3* (41%) and *MYH7* (29%) being most prevalent. There were two multiple-mutation carriers among G+LVH− and none in the G+LVH+.

Baseline CMR parameters (Table 1) for G+LVH− patients were similar to those of healthy volunteers, except for LV EF (71 ± 4 % *vs.* 69 ± 4 %, *P*=0.03), maximal septal wall thickness in systole (SWTs) (12.6 ± 3.2 mm *vs.* 11.2 ± 2.1 mm, *P*=0.03), end-systolic volume (ESV) (38 ± 9 mls *vs.* 43 ± 12 mls, *P*=0.03) and AMVL length (23.5 ± 3.0 mm *vs.* 19.7 ± 3.1 mm; *P*<0.0001). Substantial differences in CMR parameters were observed between G+LVH+/G–LVH+ HCM patients and healthy matched volunteers.

In G+LVH+ and G–LVH+ patients, asymmetric septal hypertrophy was the commonest pattern of LVH (84% and 61% respectively). Resting peak left ventricular outflow tract obstruction and systolic anterior motion of the mitral valve were observed in 39% and 52% of G+LVH+ cases respectively and in 33% and 42% of G–LVH+. Delayed contrast enhancement was present in 90% of G+LVH+ (28/31) and in 81% of G–LVH+ (29/36) but was absent in all G+LVH− patients and healthy volunteers.

Trabeculation

G+LVH− patients had increased global LV trabecular complexity compared to healthy volunteers (1.176 ± 0.06 *vs.* 1.149 ± 0.03, *P*=0.01). This was most marked in the apical half of the LV (maximal apical FD, 1.249 ± 0.07 *vs.* 1.199 ± 0.05, *P*=0.001). In this case-control population, the optimum threshold value for maximal apical FD, that distinguished G+LVH− patients from healthy volunteers, was found to be ≥1.241. We found no difference in trabecular complexity between G+LVH− patients and controls in the basal half of the LV (*P*=0.21, *P*=0.97, for mean and maximal basal FD) (Figures 3 and 4A; Table 2). In G+LVH− patients there was no difference in trabeculation between those with a Romhilt-Estes ECG score of 1-3 *vs.* 0 (6/39 *vs.* 33/39; *P*=0.62).

G+LVH+ and G−LVH+ patients had elevated FD across the whole LV compared to healthy volunteers (*P*<0.0001 for all comparisons, Figures 4B and 4C; Table 2). In G+LVH− patients maximal apical FD showed weak positive relationships with maximal diastolic (*r*=0.41, *P*=0.01; Figure 5) and systolic septal wall thickness (*r*=0.42, *P*=0.01), and LV mass-index (*r*=0.33, *P*=0.04); and a weak negative relationship with gender (*r*=-0.33, *P*=0.04). In G+LVH+ and G−LVH+ patients, FD was negatively correlated with BSA, LV end-diastolic volume (*r*=-0.25, *P*=0.04) and stroke volume and positively correlated with LV mass-index, EF, wall thickness and presence of scar (for scar, *r*=0.24, *P*=0.047).

Relation of gene status to trabeculae and anterior mitral valve leaflet morphology

In patients with LVH, univariate analysis identified age, ethnicity, gender, BSA, LV mass, maximal systolic and diastolic septal and posterior wall thickness, left atrial size and presence of delayed contrast enhancement as being associated with maximal apical FD and AMVL length. After adjusting for these factors trabeculation and AMVL length did not differ significantly between G+LVH+ and G−LVH+ patients (maximal apical FD, B=-0.01, *P*=0.90; AMVL length, B=0.22, *P*=0.07) and no gene-specific differences in trabeculation were observed in G+LVH+ and G+LVH− patients (*MYBPC3 vs. MYH7* mutations, B=0.16, *P*=0.24; thick *vs.* thin filament mutations, B=-0.04, *P*=0.66).

Relation of trabeculae to myocardial clefts

Myocardial clefts were commoner in G+LVH− patients (11/39, 28%) compared to healthy volunteers (3/39, 8%; *P*=0.02). Of the 11 G+LVH− patients with clefts, 50% had >1 cleft (2 or 3) whereas all healthy volunteers had singular clefts. Clefts predominated in the basal inferior and inferoseptal walls. Within the G+LVH− group maximal apical FD did not differ significantly in the presence or absence of clefts (maximal apical FD, 1.256 ± 0.02 *vs.* 1.246 ± 0.01 respectively, *P*=0.71).

Discussion

These data show that carriers of HCM causing mutations with no LVH or scar have abnormal apical trabeculation. Three other previously described morphological abnormalities (myocardial clefts, AMVL elongation, increased systolic wall thickening) were also more common in mutation carriers. Together, these findings represent a preclinical HCM phenotype.[7,21,22]

HCM patients have a lifelong risk of heart failure, atrial fibrillation, stroke, and sudden cardiac death.[23] Detection of a preclinical HCM phenotype[24–26] in the relatives of probands, facilitates closer clinical surveillance[27] and may provide a surrogate marker for future therapeutic trials.[28] In spite of this refined description of the intermediate HCM phenotype, detailed cardiac imaging studies are still unable to reliably distinguish preclinical HCM subjects from normal G− relatives on the basis of cardiac morphology alone,[26] calling for the study of larger G+LVH− populations and direct comparison with G− relatives.

In this study, endocardial contours in the apical half of the LV were mathematically more complex in G+LVH− patients when compared to healthy volunteers. The finding of increased apical trabeculation in HCM is therefore one (new) of several (known) phenotypic abnormalities that have been described in gene mutation carriers before the development of hypertrophy. The trabecular abnormalities were more pronounced (higher FD) and widespread (also involving the base) in patients with LVH irrespective of genetic status.

Trabeculae are composed of sheets of cardiomyocytes[29] lined by endocardial cells. They form at the end of human gestational week-4[30] and their subsequent maturation is governed by genetic factors. Mutations of genes encoding NOTCH signaling pathway regulators,[31] sarcomeric,[32] cytoskeletal,[33] nuclear-membrane[34] and chaperone proteins[35] have been implicated in the trabecular disarray that results in left ventricular noncompaction. In HCM carriers it is therefore plausible that the interplay of the primary genetic defect and environmental factors[36] may also be influencing trabecular formation. Trabecular thickening occurs in LVH[37] and must account for some of the increased fractal complexity seen in our HCM cases (with some contribution from hypertrophied papillary muscles). In G+LVH− patients trabecular abnormalities are picked up by fractal analysis, even when other more conventional metrics (end-diastolic wall thickness, LV mass, ECG surrogates) fail to show clinically appreciable hypertrophy. Clefts are commoner in G+LVH− but they do not explain the FD increase as their presence was not associated with FD and they are more basal[8] and less visible on the short-axis slices.

We observed higher EF and SWTs and smaller ESV in our G+LVH− cohort compared to healthy volunteers. Elevated EF[38–40] and hypercontractility[41] have been previously documented, but diastolic[42] and systolic dysfunction[43] have also been seen, although the latter may have been due to myocardial scar[43] whereas our carriers were entirely free of scar. Elongation of the AMVL was also confirmed.[5] The precise mechanism for this is not known but sarcomeric protein mutations may influence valvulogenesis through abnormal fibroblastic differentiation of epicardial-derived cells[44] adjacent to the mitral valve which increase levels of periostin,[45] thought to be important in the regulation of valve differentiation and maturation.[46] Longitudinal, morphological study of HCM animal models bearing sarcomere mutations that cause the human disease, could improve our understanding of phenotype evolution in preclinical and overt HCM, distinguishing the primary effects of sarcomere mutations from other compensatory structural changes.[26] Just as in humans where age-dependent penetrance of HCM is seen, these published animal models (Table 3) only start to express LVH or histological changes typical for hypertrophy, later on in life. It is still unknown

whether the preclinical abnormalities described in the human G+LVH− hearts are similarly recapitulated in these murine HCM mutants.

Limitations of this study are that it is single-centre and cross-sectional in design. Some G+LVH− patients were related and trabecular morphology in family members of G−LVH+ HCM probands and in those of G+LVH+/− probands has not been evaluated. Results found in the carrier population merit validation in a separate, external G+LVH− cohort.

Conclusions

Increased myocardial trabecular complexity is one of several other phenotypic abnormalities that can be identified by CMR in HCM sarcomere gene mutation carriers without LVH.

Acknowledgements

All authors have contributed significantly to the submitted work: J.C.M. and P.M.E. conceived and directed the project. G.C wrote the article. V.Mu., C.L and G.C. developed the CMR trabecular fractal analysis toolkit. L.L. was involved in the analysis and interpretation of the next generation sequencing genotype data. P.S. was involved in the experimental design and execution of next generation sequencing methods and the analysis and interpretation of sequencing data. G.C., D.S., V.M. and J.C.M. performed the CMR imaging in humans. V.P. and G.C. recruited the study participants. G.C., L.L. and V.P. analyzed the human data. P.M.E, V.Mu., L.L., P.B., T.J.M., C.L., P.S. and W.J.M. provided expert advice and critical review of the manuscript. All authors read and approved the final manuscript.

Funding Sources

Dr Moon: Higher Education Funding Council for England; Prof Elliott: British Heart Foundation, NIHR, unrestricted educational grants Genzyme and Shire; Dr Captur: University College London Graduate Research Grant, Charlotte and Yule Bogue Research Fellowship and European Union

Science and Technology Research Grant; Dr Lopes: Grant from the Gulbenkian Doctoral Programme for Advanced Medical Education, sponsored by Fundação Calouste Gulbenkian, Fundação Champalimaud, Ministério da Saúde and Fundação para a Ciência e Tecnologia, Portugal. Dr Muthurangu: British Heart Foundation. This work was undertaken at the University College London Hospital and University College London, which receive a proportion of funding from the Department of Health's National Institute for Health Research Biomedical Research Centres funding scheme.

Disclosures

The authors declare that they have no competing interests.

References

1. Maron MS. Clinical Utility of Cardiovascular Magnetic Resonance in Hypertrophic Cardiomyopathy. *J Cardiovasc Mag Res*. 2012; 14:12–15.

2. Elliott P, Andersson B, Arbustini E, Bilinska Z, Cecchi F, Charron P, Dubourg O, Kühl U, Maisch B, McKenna WJ, Monserrat L, Pankuweit S, Rapezzi C, Seferovic P, Tavazzi L, Keren A. Classification of the cardiomyopathies: a position statement from the European Society Of Cardiology Working Group on Myocardial and Pericardial Diseases. *Eur Heart J*. 2008; 29:270–6.

3. Pezzoli L, Sana ME, Ferrazzi P, Iascone M. A new mutational mechanism for hypertrophic cardiomyopathy. *Gene*. 2012; 507:165–9.

4. Page SP, Kounas S, Syrris P, Christiansen M, Frank-Hansen R, Andersen PS, Elliott PM, McKenna WJ. Cardiac myosin binding protein-C mutations in families with hypertrophic cardiomyopathy: disease expression in relation to age, gender, and long term outcome. *Circ Cardiovasc Genet*. 2012; 5:156–66.

5. Maron MS, Olivotto I, Harrigan C, Appelbaum E, Gibson CM, Lesser R, Haas TS, Udelson JE, Manning WJ, Maron BJ. Mitral valve abnormalities identified by cardiovascular magnetic resonance represent a primary phenotypic expression of hypertrophic cardiomyopathy. *Circ*. 2011; 124:40–47.

6. Johansson B, Maceira AM, Babu-Narayan S V, Moon JC, Pennell DJ, Kilner PJ. Clefts can be seen in the basal inferior wall of the left ventricle and the interventricular septum in healthy volunteers as well as patients by cardiovascular magnetic resonance. *J Am Coll Cardiol*. 2007; 50:1294–5.

7. Moon JC, McKenna WJ. Myocardial crypts: a prephenotypic marker of hypertrophic cardiomyopathy? *Circ Cardiovasc Imaging*. 2012; 5:431–2.

8. Deva DP, Williams LK, Care M, Siminovitch KA, Moshonov H, Wintersperger BJ, Rakowski H, Crean AM. Deep basal inferoseptal crypts occur more commonly in patients with hypertrophic cardiomyopathy due to disease-causing myofilament mutations. *Radiology*. 2013; Jun 14.

9. Noureldin RA, Liu S, Nacif MS, Judge DP, Halushka MK, Abraham TP, Ho C, Bluemke DA. The diagnosis of hypertrophic cardiomyopathy by cardiovascular magnetic resonance. *J Cardiovasc Magn Reson*. 2012; 14:17.

10. Grothoff M, Pachowsky M, Hoffmann J, Posch M, Klaassen S, Lehmkuhl L, Gutberlet M. Value of cardiovascular MR in diagnosing left ventricular non-compaction cardiomyopathy and in discriminating between other cardiomyopathies. *Eur Radiol*. 2012; 22:2699–709.

11. Petersen SE, Selvanayagam JB, Wiesmann F, Robson MD, Francis JM, Anderson RH, Watkins H, Neubauer S. Left ventricular non-compaction: insights from cardiovascular magnetic resonance imaging. *J Am Coll Cardiol*. 2005; 46:101–5.

12. Captur G, Muthurangu V, Cook C, Flett AS, Wilson R, Barison A, Sado DM, Anderson S, McKenna WJ, Mohun TJ, Elliott PM, Moon JC. Quantification of left ventricular trabeculae using fractal analysis. *J Cardiovasc Magn Reson*. 2013; 15:36.

13. Konno T, Shimizu M, Ino H, Fujino N, Hayashi K, Uchiyama K, Kaneda T, Inoue M, Fujita T, Masuta E, Funada A, Mabuchi H. Differences in diagnostic value of four electrocardiographic voltage criteria for hypertrophic cardiomyopathy in a genotyped population. *Am J Cardiol*. 2005; 96:1308–12.

14. Charron P. Accuracy of European diagnostic criteria for familial hypertrophic cardiomyopathy in a genotyped population. *Int J Cardiol*. 2003; 90:33–38.

15. McKenna WJ, Spirito P, Desnos M, Dubourg O, Komajda M. Experience from clinical genetics in hypertrophic cardiomyopathy: proposal for new diagnostic criteria in adult members of affected families. *Heart*. 1997; 77:130–2.

16. Lopes LR, Zekavati A, Syrris P, Hubank M, Giambartolomei C, Dalageorgou C, Jenkins S, McKenna W, Plagnol V, Elliott PM. Genetic complexity in hypertrophic cardiomyopathy revealed by high-throughput sequencing. *J Med Genet*. 2013; 50:228–39.

17. Abecasis GR, Auton A, Brooks LD, DePristo MA, Durbin RM, Handsaker RE, Kang HM, Marth GT, McVean GA. An integrated map of genetic variation from 1,092 human genomes. *Nature*. 2012; 491:56–65.

18. Kramer CM, Barkhausen J, Flamm SD, Kim RJ, Nagel E. Standardized cardiovascular magnetic resonance imaging (CMR) protocols, society for cardiovascular magnetic resonance: board of trustees task force on standardized protocols. *J Cardiovasc Magn Reson*. 2008; 10:35.

19. Alfakih K, Plein S, Thiele H, Jones T, Ridgway JP, Sivananthan MU. Normal human left and right ventricular dimensions for MRI as assessed by turbo gradient echo and steady-state free precession imaging sequences. *J Magn Reson Imaging*. 2003; 17:323–9.

20. Li C, Huang R, Ding Z, Gatenby JC, Metaxas DN, Gore JC. A level set method for image segmentation in the presence of intensity inhomogeneities with application to MRI. *IEEE Trans Image Process*. 2011; 20:2007–16.

21. Ho CY, Abbasi SA, Neilan TG, Shah R V, Chen Y, Heydari B, Cirino AL, Lakdawala NK, Orav EJ, González A, López B, Díez J, Jerosch-Herold M, Kwong RY. T1 measurements identify extracellular volume expansion in hypertrophic cardiomyopathy sarcomere mutation carriers with and without left ventricular hypertrophy. *Circ Cardiovasc Imaging*. 2013; 6:415–422.

22. Ho CY, López B, Coelho-Filho OR, Lakdawala NK, Cirino AL, Jarolim P, Kwong R, González A, Colan SD, Seidman JG, Díez J, Seidman CE. Myocardial fibrosis as an early manifestation of hypertrophic cardiomyopathy. *N Engl J Med*. 2010; 363:552–63.

23. Lopes LR, Rahman MS, Elliott PM. A systematic review and meta-analysis of genotype-phenotype associations in patients with hypertrophic cardiomyopathy caused by sarcomeric protein mutations. *Heart*. 2013;:1–12.

24. Gray B, Ingles J, Semsarian C. Natural history of genotype positive-phenotype negative patients with hypertrophic cardiomyopathy. *Int J Cardiol*. 2011; 152:258–9.

25. Maron BJ, Semsarian C. Emergence of gene mutation carriers and the expanding disease spectrum of hypertrophic cardiomyopathy. *Eur Heart J*. 2010; 31:1551–3.

26. Ho CY. Hypertrophic cardiomyopathy: preclinical and early phenotype. *J Cardiovasc Transl Res*. 2009; 2:462–70.

27. Christiaans I, Lekanne dit Deprez RH, Van Langen IM, Wilde AAM. Ventricular fibrillation in MYH7-related hypertrophic cardiomyopathy before onset of ventricular hypertrophy. *Heart Rhythm*. 2009; 6:1366–9.

28. Maron BJ, Maron MS, Semsarian C. Genetics of hypertrophic cardiomyopathy after 20 years: clinical perspectives. *J Am Coll Cardiol*. 2012; 60:705–15.

29. Sedmera D, Pexieder T, Vuillemin M, Thompson RP, Anderson RH. Developmental patterning of the myocardium. *Anat Rec*. 2000; 258:319–37.

30. Towbin JA. Left ventricular noncompaction: a new form of heart failure. *Heart Fail Clin*. 2010; 6:453–69.

31. Luxán G, Casanova JC, Martínez-Poveda B, Prados B, D'Amato G, MacGrogan D, Gonzalez-Rajal A, Dobarro D, Torroja C, Martinez F, Izquierdo-García JL, Fernández-Friera L, Sabater-Molina M, Kong Y-Y, Pizarro G, Ibañez B, Medrano C, García-Pavía P, Gimeno JR, Monserrat L, Jiménez-Borreguero LJ, De la Pompa JL. Mutations in the NOTCH pathway regulator MIB1 cause left ventricular noncompaction cardiomyopathy. *Nat Med*. 2013; 19:193–201.

32. Klaassen S, Probst S, Oechslin E, Gerull B, Krings G, Schuler P, Greutmann M, Hürlimann D, Yegitbasi M, Pons L, Gramlich M, Drenckhahn J-D, Heuser A, Berger F, Jenni R, Thierfelder L. Mutations in sarcomere protein genes in left ventricular noncompaction. *Circ*. 2008; 117:2893–901.

33. Ichida F, Tsubata S, Bowles KR, Haneda N, Uese K, Miyawaki T, Dreyer WJ, Messina J, Li H, Bowles NE, Towbin JA. Novel gene mutations in patients with left ventricular noncompaction or Barth syndrome. *Circ*. 2001; 103:1256–63.

34. Hermida-Prieto M, Monserrat L, Castro-Beiras A, Laredo R, Soler R, Peteiro J, Rodríguez E, Bouzas B, Alvarez N, Muñiz J, Crespo-Leiro M. Familial dilated cardiomyopathy and isolated left ventricular noncompaction associated with lamin A/C gene mutations. *Am J Cardiol*. 2004; 94:50–4.

35. Shou W, Aghdasi B, Armstrong DL, Guo Q, Bao S, Charng MJ, Mathews LM, Schneider MD, Hamilton SL, Matzuk MM. Cardiac defects and altered ryanodine receptor function in mice lacking FKBP12. *Nature*. 1998; 391:489–92.

36. Olivotto I, Girolami F, Nistri S, Rossi A, Rega L, Garbini F, Grifoni C, Cecchi F, Yacoub MH. The many faces of hypertrophic cardiomyopathy: from developmental biology to clinical practice. *J Cardiovasc Transl Res*. 2009; 2:349–67.

37. Ueno H, Yokota Y, Yokoyama M IH. Comparison of echocardiographic and anatomic measurements of the left ventricular wall thickness. *Kobe J Med Sci*. 1991; 37:273–86.

38. De S, Borowski AG, Wang H, Nye L, Xin B, Thomas JD, Tang WHW. Subclinical echocardiographic abnormalities in phenotype-negative carriers of myosin-binding protein C3 gene mutation for hypertrophic cardiomyopathy. *Am Heart J*. 2011; 162:262–267.e3.

39. Lakdawala NK, Thune JJ, Maron BJ, Cirino AL, Havndrup O, Bundgaard H, Christiansen M, Carlsen CM, Dorval J-F, Kwong RY, Colan SD, Køber L V, Ho CY. Electrocardiographic features of sarcomere mutation carriers with and without clinically overt hypertrophic cardiomyopathy. *Am J Cardiol*. 2011; 108:1606–13.

40. Ho C, Sweitzer N, McDonough B, Maron B, Casey S, Seidman J, Seidman C, Solomon S. Assessment of diastolic function with doppler tissue imaging to predict genotype in preclinical hypertrophic cardiomyopathy. *Circ*. 2002; 105:2992–7.

41. Devlin A, Ostman-Smith I. Diagnosis of hypertrophic cardiomyopathy and screening for the phenotype suggestive of gene carriage in familial disease : a simple echocardiographic procedure. *J Med Screen.* 2000; 7:82–90.

42. Kauer F, Van Dalen BM, Michels M, Soliman OII, Vletter WB, Van Slegtenhorst M, Ten Cate FJ, Geleijnse ML. Diastolic abnormalities in normal phenotype hypertrophic cardiomyopathy gene carriers: a study using speckle tracking echocardiography. *Echocardiography*. 2013; 30:558–63.

43. Germans T, Rüssel IK, Götte MJW, Spreeuwenberg MD, Doevendans P a, Pinto YM, Van der Geest RJ, Van der Velden J, Wilde AAM, Van Rossum AC. How do hypertrophic cardiomyopathy mutations affect myocardial function in carriers with normal wall thickness? Assessment with cardiovascular magnetic resonance. *J Cardiovasc Magn Reson*. 2010; 12:13.

44. Rajan S, Williams SS, Jagatheesan G, Ahmed RPH, Fuller-Bicer G, Schwartz A, Aronow BJ, Wieczorek DF. Microarray analysis of gene expression during early stages of mild and severe cardiac hypertrophy. *Physiol Genomics*. 2006; 27:309–17.

45. Markwald RR, Norris RA, Moreno-rodriguez R, Levine RA. Developmental basis of adult cardiovascular diseases: valvular heart diseases. 2010; 1188:177–183.

46. Niu Z, Iyer D, Conway SJ, Martin JF, Ivey K, Srivastava D, Nordheim A, Schwartz RJ. Serum response factor orchestrates nascent sarcomerogenesis and silences the biomineralization gene program in the heart. *Proc Natl Acad Sci U S A*. 2008; 105:17824–9.

47. Shephard R, Semsarian C. Role of animal models in HCM research. *J Cardiovasc Transl Res*. 2009; 2:471–82.

48. Vignier N, Schlossarek S, Fraysse B, Mearini G, Krämer E, Pointu H, Mougenot N, Guiard J, Reimer R, Hohenberg H, Schwartz K, Vernet M, Eschenhagen T, Carrier L. Nonsense-mediated mRNA decay and ubiquitin-proteasome system regulate cardiac myosin-binding protein C mutant levels in cardiomyopathic mice. *Circ Res*. 2009; 105:239–48.

49. McConnell BK, Fatkin D, Semsarian C, Jones K a., Georgakopoulos D, Maguire CT, Healey MJ, Mudd JO, Moskowitz IPG, Conner D a., Giewat M, Wakimoto H, Berul CI, Schoen FJ, Kass D a., Seidman CE, Seidman JG. Comparison of Two Murine Models of Familial Hypertrophic Cardiomyopathy. *Circulation Research*. 2001; 88:383–389.

50. Carrier L, Knöll R, Vignier N, Keller DI, Bausero P, Prudhon B, Isnard R, Ambroisine M-L, Fiszman M, Ross J, Schwartz K, Chien KR. Asymmetric septal hypertrophy in heterozygous cMyBP-C null mice. *Cardiovasc Res*. 2004; 63:293–304.

51. Tardiff JC, Factor SM, Tompkins BD, Hewett TE, Palmer BM, Moore RL, Schwartz S, Robbins J, Leinwand L a. A truncated cardiac troponin T molecule in transgenic mice suggests multiple cellular mechanisms for familial hypertrophic cardiomyopathy. *J Clin Invest*. 1998; 101:2800–11.

52. Javadpour MM, Tardiff JC, Pinz I, Ingwall JS. Decreased energetics in murine hearts bearing the R92Q mutation in cardiac troponin T. 2003; 112.

53. Tsoutsman T, Chung J, Doolan A, Nguyen L, Williams I a, Tu E, Lam L, Bailey CG, Rasko JEJ, Allen DG, Semsarian C. Molecular insights from a novel cardiac troponin I mouse model of familial hypertrophic cardiomyopathy. *J Mol Cell Cardiol*. 2006; 41:623–32.

54. James J, Zhang Y, Osinska H, Sanbe a., Klevitsky R, Hewett TE, Robbins J. Transgenic Modeling of a Cardiac Troponin I Mutation Linked to Familial Hypertrophic Cardiomyopathy. *Circulation Research*. 2000; 87:805–811.

55. Geisterfer-lowrance AAAT, Christe M, Conner DA, Joanne S, Schoen FJ, Seidman CE, Seidman JG, Science S, Series N, May N. A Mouse Model of Familial Hypertrophic Cardiomyopathy. 2013; 272:731–734.

56. Jones WK, Grupp IL, Doetschman T, Grupp G, Osinska H, Hewett TE, Boivin G, Gulick J, Ng W a, Robbins J. Ablation of the murine alpha myosin heavy chain gene leads to dosage effects and functional deficits in the heart. *J Clin Invest*. 1996; 98:1906–17.

57. Muthuchamy M, Pieples K, Rethinasamy P, Hoit B, Grupp IL, Boivin GP, Wolska B, Evans C, Solaro RJ, Wieczorek DF. Mouse Model of a Familial Hypertrophic Cardiomyopathy Mutation in -Tropomyosin Manifests Cardiac Dysfunction. *Circulation Research*. 1999; 85:47–56.

58. Prabhakar R, Boivin GP, Grupp IL, Hoit B, Arteaga G, Solaro RJ, Wieczorek DF. A familial hypertrophic cardiomyopathy alpha-tropomyosin mutation causes severe cardiac hypertrophy and death in mice. *J Mol Cell Cardiol*. 2001; 33:1815–28.

59. Tsoutsman T, Kelly M, Ng DCH, Tan J-E, Tu E, Lam L, Bogoyevitch M a, Seidman CE, Seidman JG, Semsarian C. Severe heart failure and early mortality in a double-mutation mouse model of familial hypertrophic cardiomyopathy. *Circ*. 2008; 117:1820–31.

Tables

Table 1 Baseline characteristics and CMR parameters.

Variable	**G+LVH−** (***n*=39***)	**Normals** (***n*=39**)	***P*‡**	**G+LVH+** (***n*=31**)	**Normals** (***n*=31**)	***P*‡**	**G−LVH+** (***n*=36**)	**Normals** (***n*=36**)	***P*‡**
Age (yrs)	33±15	37±12	0.094	47±12	45±14	0.667	57±15	51±15	0.085
Male/Female	15/24	15/24	NS	19/12	19/12	NS	32/4	32/4	NS
Ethnicity†	A=38 D=1	A=38 D=1	NS	A=21 C=2 D=5 E=3	A=21 C=2 D=5 E=3	NS	A=25 C=8 D=2 E=1	A=25 C=8 D=2 E=1	NS
BSA (m^2)	1.8±0.2	1.8±0.2	0.544	1.9±0.2	1.9±0.2	0.916	2.0±0.2	2.0±0.2	0.801
LVEDV (mls)	129±23	136±25	0.213	144±46	140±23	0.642	130±34	145±23	**0.026**
LVEDV*i* (mls/m^2)	72±10	74±11	0.315	74±22	72±9	0.656	66±15	73±9	**0.018**
LVESV(mls)	38±9	43±12	**0.033**	43±30	45±10	0.789	32±17	47±12	**<0.0001**
LVESV*i* (mls/m^2)	21±4	24±6	**0.039**	22±15	23±5	0.777	16±8	24±5	**<0.0001**
EF (%)	71±4	68±4	**0.034**	71±10	68±5	0.129	76±9	67±4	**<0.0001**
Mass (g)	108±32	108±31	1.0	226±98	127±37	**<0.0001**	262±113	141±30	**<0.0001**
Mass*i* (g/m^2)	60±13	59±14	0.849	117±51	65±14	**<0.0001**	133±59	71±14	**<0.0001**
SV (mls)	91±16	92±16	0.717	100±29	95±18	0.352	98±25	97±15	0.821
SWTd (mm)	9.1±1.9	8.5±1.2	0.075	21.0±6.5	9.0±1.4	**<0.0001**	21.3±5.4	9.8±1.3	**<0.0001**
PWTd (mm)	6.5±1.4	6.5±1.4	0.945	9.7±3.2	7.06±1.6	**<0.001**	12.7±4.3	7.3±1.5	**<0.0001**
SWTs (mm)	12.6±3.2	11.2±2.1	**0.031**	24.7±5.8	12.3±2.7	**<0.0001**	26.7±5.0	12.9±2.6	**<0.0001**
PWTs (mm)	12.3±2.8	11.9±2.5	0.457	17.8±3.8	12.7±2.8	**<0.0001**	20.9±5.0	13.4±2.9	**<0.0001**
SdPdR	1.4±0.3	1.4±0.3	0.338	2.3±1.0	1.3±0.3	**<0.0001**	1.8±0.6	1.4±0.3	**0.002**
SsSdR	1.4±0.2	1.3±0.3	0.320	1.2±0.2	1.4±0.3	**0.02**	1.3±0.3	1.3±0.2	0.798
PsPdR	1.9±0.4	1.8±0.3	0.317	1.9±0.4	1.8±0.3	0.382	1.7±0.4	1.9±0.3	0.149
LA area (cm^2)	19.5±3.4	19.3±2.7	0.761	29.6±6.5	19.4±2.7	**<0.0001**	27.1±7.0	19.6±2.6	**<0.0001**
LA area*i* (cm^2/m^2)	10.8±1.5	10.6±1.4	0.394	15.3±3.4	10.0±1.2	**<0.0001**	13.7±3.4	10.0±1.4	**<0.0001**
AMVL (mm)	23.5±3.0	19.7±3.1	**<0.0001**	24.6±4.6	19.6±2.8	**<0.0001**	25.7±3.3	19.2±3.0	**<0.0001**

*After exclusion of 1 case with left ventricular hypertrophy detected by CMR.

†Ethnic headings are defined in accordance with UK Office for National Statistics guidance on national standards: A = White; B = Mixed; C = Asian or Asian Black; D = Black or Black British; E = Chinese or other ethnic group (including Arab).

‡Significant *P* values are highlighted in bold.

AMVL, anterior mitral valve leaflet length; BSA, body surface area; CMR, cardiovascular magnetic resonance; EF, ejection fraction; G+/G−, sarcomere gene mutation positive/negative; LA area*i*, left atrial area indexed to BSA; LVEDV*i*, left ventricular end-diastolic volume indexed to BSA; LVESV*i*, left ventricular end-systolic volume indexed to BSA; LVH+/LVH−, left ventricular hypertrophy present/absent; Mass*i*, LV mass indexed to BSA; NS, not significant; PsPdR, systolic posterior to diastolic posterior wall thickness ratio; PWTd/s, maximal posterior wall thickness in diastole/systole; s.d., standard deviation; SdPdR, diastolic septal to diastolic posterior wall thickness ratio; SsSdR, systolic septal to diastolic septal wall thickness ratio; SV, stroke volume; SWTd/s, maximal septal wall thickness in diastole/systole; yrs, years.

Table 2 Fractal dimensions across all populations.

FD	G+LVH− (*n*=39*)	Normals (*n*=39†)	*P*‖	G+LVH+ (*n*=31)	Normals (*n*=31‡)	*P*‖	G−LVH+ (*n*=36)	Normals (*n*=36§)	*P*‖
Mn. Basal	1.142±0.07	1.126±0.04	0.213	1.255±0.07	1.138±0.06	**<0.0001**	1.219±0.07	1.130±0.07	**<0.0001**
Max. Basal	1.218±0.08	1.217±0.05	0.973	1.344±0.08	1.227±0.05	**<0.0001**	1.305±0.09	1.223±0.06	**<0.0001**
Global LV	1.176±0.06	1.149±0.03	**0.012**	1.300±0.06	1.165±0.05	**<0.0001**	1.279±0.07	1.169±0.05	**<0.0001**
Mn. Apical	1.202±0.07	1.162±0.05	**0.006**	1.332±0.08	1.179±0.06	**<0.0001**	1.327±0.08	1.196±0.06	**<0.0001**
Max. Apical	1.249±0.07	1.199±0.05	**0.001**	1.370±0.08	1.211±0.06	**<0.0001**	1.380±0.09	1.232±0.06	**<0.0001**

*After exclusion of 1 case with LVH detected by CMR.

†Of which non-White, *n* = 1 (ethnically matched to G+LVH−)

‡Of which non-White, *n* = 10 (ethnically matched to G+LVH+)

§Of which non-White, *n* = 11 (ethnically matched to G−LVH+)

‖Significant *P* values are highlighted in bold.

FD, fractal dimension; Max., maximal; Mn., mean; Other abbreviations as in Table 1.

Table 3 Murine models for HCM[47] published to date.

Gene Family	Published	Mutation detail	Postnatal Phenotype
MYBPC3	Vignier et al.[48] 2009	Knockin	Ho-KI show LVH, ↓FS, interstitial fibrosis >3mo Het-KI showed no major phenotype
	McConnell et al.[49] 2001	Truncated	Het show slight LVH by 30wk
	Carrier et al.[50] 2004	Knockout	Ho show eccentric LVH, ↓FS >3mo; ↓relaxation >9mo Het show ASH, interstitial fibrosis >10mo
TNNT	Tardiff et al.[51] 1998	Truncated	↓LV mass by 4mo, impaired relaxation
	Javadpour et al.[52] 2003	R92Q	↓LV mass, impaired relaxation
TNNI	Tsoutsman et al.[53] 2006	G203S	LVH, interstitial fibrosis by 21wk
	James et al.[54] 2000	R146G	Interstitial fibrosis, impaired relaxation, enhanced contractility
αMHC*	Geisterfer-Lowrance et al.[55] 1996	R403Q	Ho born with normal gross cardiac anatomy but lethal by 7 days Het show myocyte hypertrophy, interstitial fibrosis by 15wk; LVH by 30wk
	Jones et al.[56] 1996	Knockout	Ho are embryonic lethal; Het show ↓LV contractility and impaired relaxation
αTM	Muthuchamy et al.[57] 1999	D175N	↓FS , Impaired relaxation
	Prabhakar et al.[58] 2001	E180G	LVH and fibrosis by 1mo; lethal by 4mo
TNNI+αMHC	Tsoutsman et al.[59] 2008	Double-mutant: *TNNI-203/αMHC-403*	↑LV mass, interstitial fibrosis by 14 days; heart failure and lethal by 21 days

*Isoform is highly homologous to the human βMHC gene.

αMHC= alpha cardiac myosin heavy chain; αTM= alpha-tropomyosin; ASH= asymmetric septal hypertrophy; ↑= increased; ↓= decreased; FS= fractional shortening; Het= heterozygous; Ho= homozygous; KI= knock-in; mo= moths; MYBPC3= cardiac myosin-binding protein C gene; NA= not available; LVH= left ventricular hypertrophy; TNNI= cardiac troponin-I; TNNT= cardiac troponin T; wk= weeks.

Figure legends

Figure 1 Examples of preclinical HCM phenotype.

Preclinical features of HCM consisting of the presence of (A) clefts, (B) elongation of the anterior mitral valve leaflet (here 23 mm) and (C) abnormal trabeculae (here FD of 1.318). Not shown is the slightly higher contractility recorded in our cohort.

FD, fractal dimension; HCM, hypertrophic cardiomyopathy.

Figure 2 Fractal analysis for trabecular quantification.

Example analysis. A single slice (A) from a healthy volunteer cine stack. The ROI (B) is defined and the endocardial contour created using a level set method without further intervention (C). This undergoes box-counting fractal analysis (D): a series of grids of boxes of progressively smaller size are laid over the ROI and boxes containing pixel detail are counted. A natural logarithmic plot (E) of box-count (*y* axis) against scale (*x* axis, calculated from box/image size) is generated. The slope (*m*) of the line is the FD. Here, this slice has a FD of 1.257.

Ln, natural logarithm; ε, scale; ROI, region of interest. Other abbreviations as in Figure 1.

Figure 3 Mean FD values across the length of the LV from base to apex.

Mean base-to-apex interpolated FD values for the three populations (healthy volunteers, G+LVH− and G+LVH+). Heavy central lines represent mean FD values; shaded areas represent 95% confidence interval of the mean for each population.

G+, sarcomere gene mutation positive; LV, left ventricle; LVH+/−, left ventricular hypertrophy present/absent. Other abbreviations as in Figures 1 and 2.

Figure 4 Basal and apical fractal dimensions.

(A) Global LV, mean apical and maximal apical FD for G+LVH− *vs.* healthy volunteers. Global LV, maximal basal and maximal apical FD for G+LVH+ (B) and for G−LVH+ (C) *vs.* healthy volunteers. Error bars represent 95% confidence intervals. ***P*=0.012; ****P*=0.006; *****P*=0.001; †*P*<0.0001. Abbreviations as in Figures 1 and 3.

Figure 5 Relation between septal wall thickness and extent of trabeculation in G+LVH− and healthy volunteers.

Across a similar range of diastolic septal wall thicknesses, maximal apical FD tends to increase disproportionately in carriers (squares), but not in healthy volunteers (spheres) potentially reflecting the influence of sarcomere gene mutation carriership (similar findings are recorded in systole). Markers represent mean FD; error bars represent standard error of the mean.
Abbreviations as in Figures 2 and 3.

Figure 1

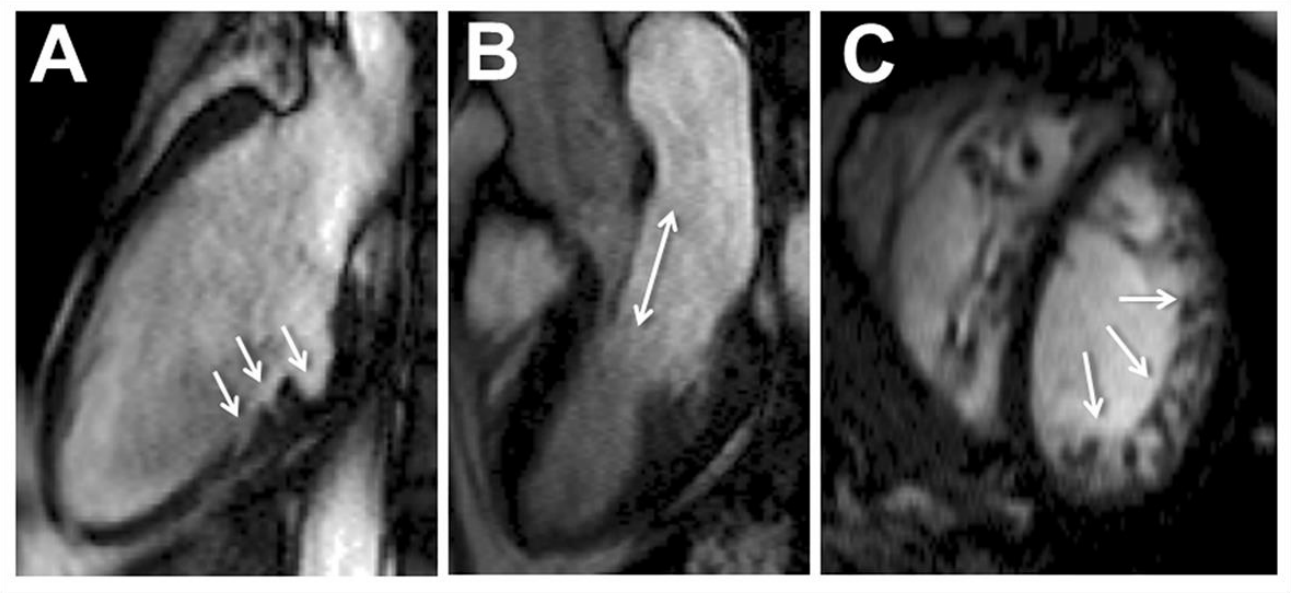

Figure 2

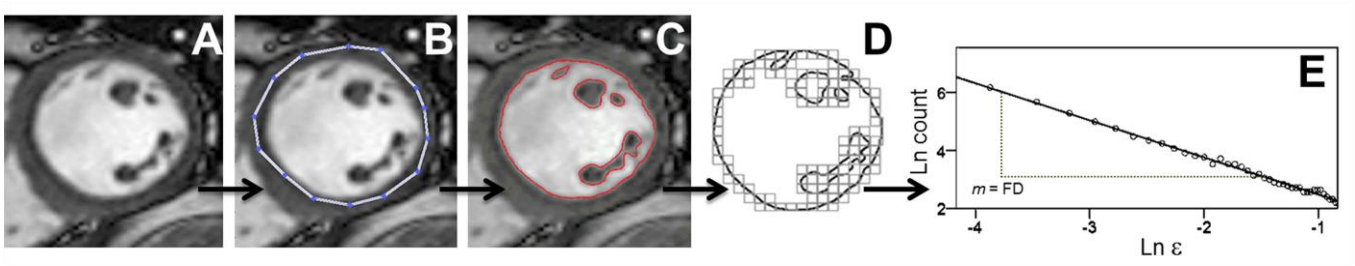

Figure 3

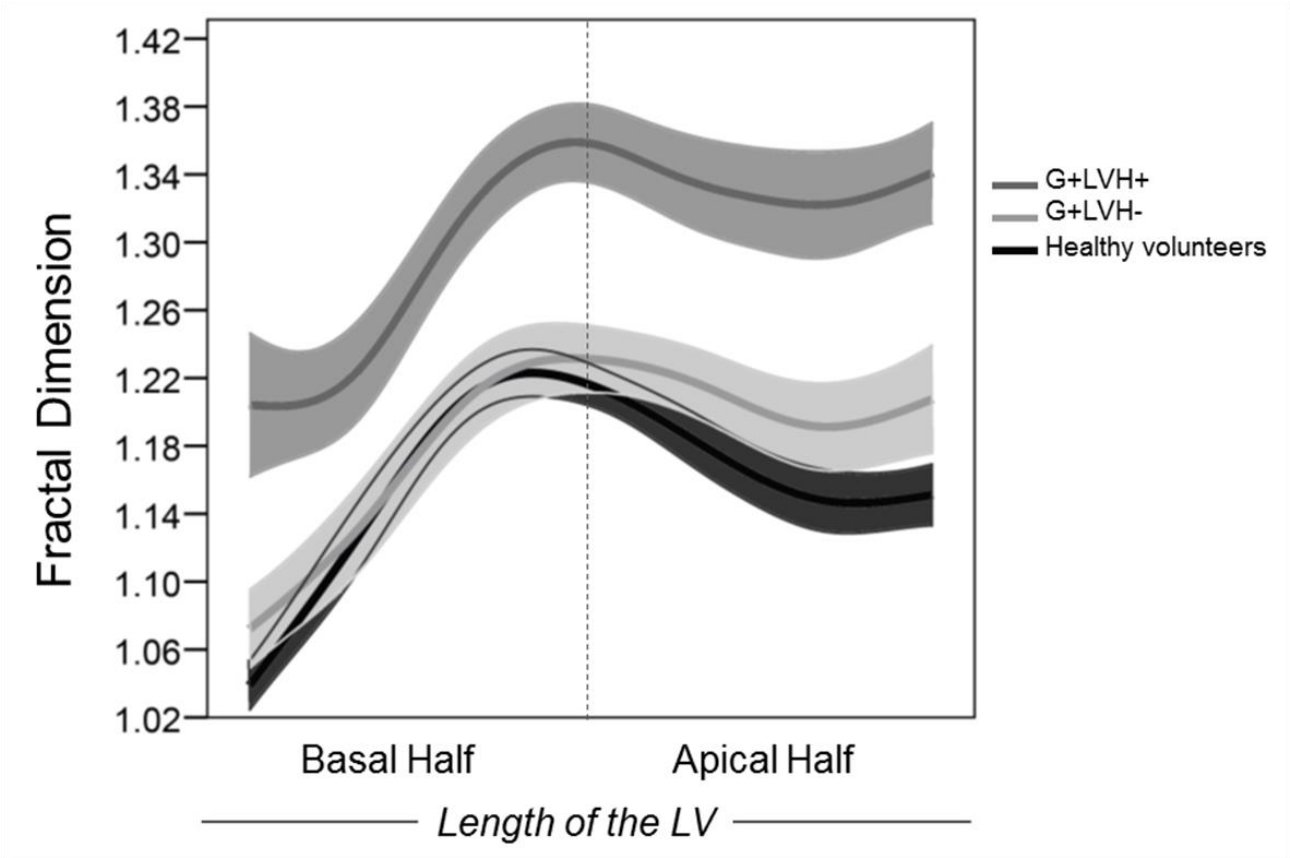
Fractal Dimension
1.42
1.38
1.34
1.30
1.26
1.22
1.18
1.14
1.10
1.06
1.02
Basal Half
Apical Half
Length of the LV
G+LVH+
G+LVH-
Healthy volunteers

Figure 4

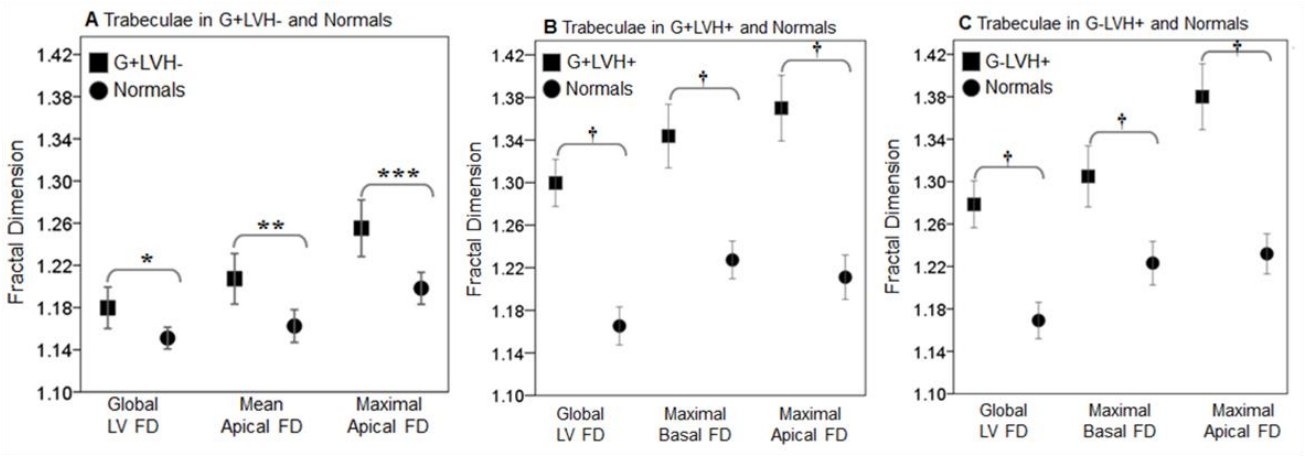
A Trabeculae in G+LVH- and Normals
G+LVH-
Normals
Fractal Dimension
1.42
1.38
1.34
1.30
1.26
1.22
1.18
1.14
1.10
*
**
***
Global LV FD
Mean Apical FD
Maximal Apical FD
B Trabeculae in G+LVH+ and Normals
G+LVH+
Normals
†
Global LV FD
Maximal Basal FD
Maximal Apical FD
C Trabeculae in G-LVH+ and Normals
G-LVH+
Normals
†
Global LV FD
Maximal Basal FD
Maximal Apical FD

Figure 5

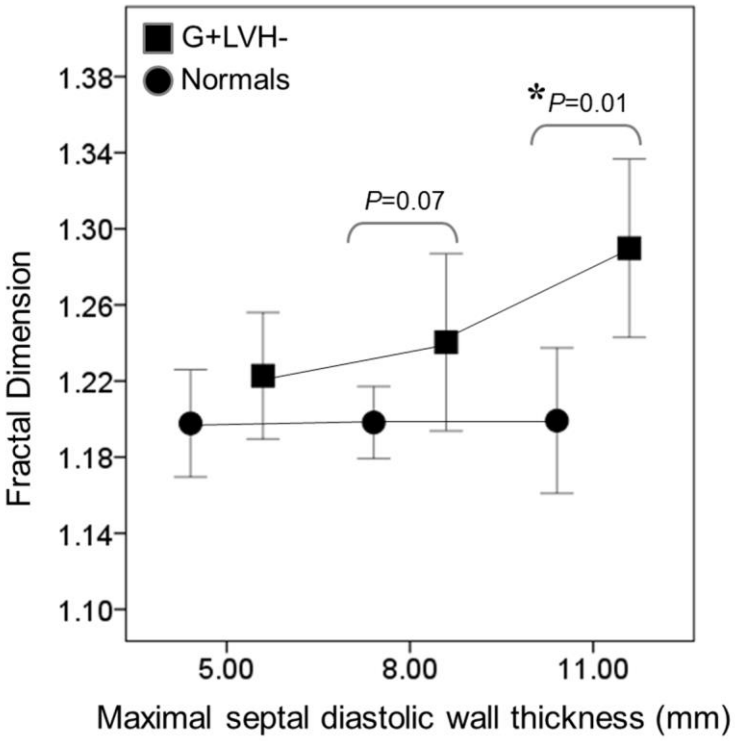
G+LVH-
Normals
*P=0.01
P=0.07
1.38
1.34
1.30
1.26
1.22
1.18
1.14
1.10
Fractal Dimension
5.00
8.00
11.00
Maximal septal diastolic wall thickness (mm)